Role of TRIM22 in ulcerative colitis and its underlying mechanisms

BIN YE[1] and ZHONGKAI LU[2]

[1]Department of Gastroenterology, Hangzhou Hospital of Traditional Chinese Medicine, Hangzhou, Zhejiang 310000; [2]Department of Gastroenterology, Suzhou Municipal Hospital, Suzhou Hospital Affiliated to Nanjing Medical University, Suzhou, Jiangsu 215001, P.R. China

Received November 2, 2021; Accepted March 16, 2022

DOI: 10.3892/mmr.2022.12765

Abstract. Ulcerative colitis (UC) is a common chronic recurrent inflammatory disease, which seriously threatens human life and health. Therefore, the present study aimed to explore the role of tripartite motif-containing (TRIM)22 in UC and its potential mechanism. C57BL/6 mice and HT-29 cell models of UC were constructed using 2% dextran sulphate sodium (DSS). The protein and mRNA expression levels were detected by western blotting and reverse transcription-quantitative PCR, respectively. Cell transfection was performed to overexpress Kruppel-like factor 2 (KLF2), or knockdown KLF2, TRIM22 and TRIM30 expression. The levels of inflammatory factors were evaluated by enzyme-linked immunosorbent assays. Cell Counting Kit-8 and TUNEL staining assay were employed to assess cell viability and apoptosis. Dual-luciferase reporter assay and chromatin immunoprecipitation assay were performed to determine the binding ability of the TRIM22 promoter to KLF2. The results revealed that DSS increased the expression levels of TRIM22 in HT-29 cells and TRIM30 in mice. Short hairpin RNA (sh)-TRIM30 could inhibit the NF-κB pathway, and reduce the levels of TNF-α, IL-6 and IFN-γ. Furthermore, KLF2 expression was downregulated in the cell model of UC, and the luciferase assay confirmed that the 3' untranslated region of TRIM22 was a direct target of KLF2. The ChIP assay also verified the binding of KLF2 with the TRIM22 promoter. Notably, knockdown of KLF2 reversed the enhancing effects of sh-TRIM22 on the viability of DSS-treated HT-29 cells. In addition, compared with in the DSS + sh-TRIM22 group, the protein expression levels of phosphorylated (p)-NF-κB and p-IκBα were increased in the DSS + sh-TRIM22 + sh-KLF2 group, as were the levels of TNF-α, IL-6 and IFN-γ. In conclusion, TRIM22 was upregulated in DSS-induced HT-29 cells. TRIM22 knockdown increased DSS-induced HT-29 cell viability and decreased apoptosis and inflammation; this was reversed by knockdown of KLF2. These findings suggested that TRIM22 may promote disease development through the NF-κB signaling pathway in UC and could be inhibited by KLF2 transcription.

Correspondence to: Dr Zhongkai Lu, Department of Gastroenterology, Suzhou Municipal Hospital, Suzhou Hospital Affiliated to Nanjing Medical University, 16 Baita West Road, Gusu, Suzhou, Jiangsu 215001, P.R. China
E-mail: luzhongkai10@126.com

Key words: ulcerative colitis, tripartite motif-containing 22, Kruppel-like factor 2, proliferation, inflammation

Introduction

Ulcerative colitis (UC) is a chronic nonspecific inflammatory bowel disease (1), the typical clinical symptoms of which are abdominal pain and diarrhea, which may contain mucus or blood (2). During the early stages, UC begins in the rectum, and in the subsequent stages it can extend to the proximal end of the colon or even the whole colon in a continuous manner, becoming a lifelong recurrent disease with a high risk of developing into colorectal cancer (3,4). Worldwide, the incidence of UC is increasing annually (5). Therefore, UC is considered one of the main diseases threatening human life and health, and the study of its potential pathogenesis is of great importance for the development of therapeutic drugs with new targets.

It has previously been reported that various genes and proteins are involved in the regulation of the progression of UC. For example, the UC-related gene RNF186 has been shown to maintain intestinal homeostasis by controlling endoplasmic reticulum stress in colonic epithelial cells (6). In addition, epithelial IL-18 equilibrium can control barrier function in colitis (7), and anti-TNF-α therapy could effectively treat UC (8). Therefore, the discovery of different molecular targeted therapies may provide a basis for the development of personalized treatment strategies to improve the treatment of patients with UC. As a subfamily of the RING type E3 ubiquitin ligases, the tripartite motif-containing (TRIM)22 protein is emerging as a key regulator in the development of various diseases by modulating transcriptional activity of the NF-κB pathway (9,10). Previous studies have reported that knockdown of TRIM22 could reduce cerebral ischemia/reperfusion-induced inflammation and apoptosis by inhibiting the NF-κB/NLRP3 axis (11), and could regulate macrophage autophagy via the NF-κB/Beclin 1 pathway (10). Notably, it has been demonstrated that functional variation of TRIM22 is related to inflammatory bowel disease (12) and may serve a

carcinogenic role in colon cancer (13). It should be noted that TRIM30 is the murine ortholog of TRIM22 (14). Therefore, the present study hypothesized that TRIM22 or TRIM30 may have a certain regulatory role in UC. The present study focused on the role and potential mechanism of TRIM30 and TRIM22 in DSS-induced UC mouse and HT-29 cell models, respectively.

Bioinformatics analysis has been widely used to explore the molecular mechanisms of various diseases (15,16), and may contribute to the identification of novel biomarkers to improve diagnostic and prognostic strategies for UC. KLF2 has been reported to be downregulated in UC, as determined by clinical information analysis, and may be closely related to inflammatory factors (17). KLF2 has also been shown to serve a regulatory role in acute lung injury as a transcription suppressor of HSPH1 (18). Therefore, it was hypothesized that TRIM22 might be inhibited by KLF2 transcription and may have a role in promoting disease development in UC. The present study investigated the effects of TRIM22 or TRIM30 on DSS-induced UC *in vivo* and *in vitro*, as well as the underlying mechanisms.

Materials and methods

Cell culture and establishment of an in vitro model of UC. The human colorectal cancer cell line HT-29, which was verified by STR profiling, was obtained from Wuhan Procell Life Science & Technology Co., Ltd. The cells were cultured in DMEM (Gibco; Thermo Fisher Scientific, Inc.) supplemented with 10% fetal bovine serum (Gibco; Thermo Fisher Scientific, Inc.). 100 U/ml penicillin and 100 μg/ml streptomycin (Gibco; Thermo Fisher Scientific, Inc.) at 37˚C in 5% CO_2. Subsequently, once HT-29 cells reached the logarithmic phase, they were inoculated into sterile 6-well plates at a density of $1x10^5$ cells/well and DSS (MilliporeSigma) was dissolved in sterile water. When cell confluence reached ~80%, cells were treated with 2% DSS or sterile water for 24 h at 37˚C to establish an *in vitro* cell model of UC.

Bioinformatics analysis. The National Center for Biotechnology Information Gene Expression Omnibus (https://www.ncbi.nlm.nih.gov/geo/) is a free public database of microarray/gene profiles, which was used to obtain the GSE59071 (19) and GSE107597 (20) in UC and normal tissue gene expression profiles (21). GEO2R (ncbi.nlm.nih.gov/geo/geo2r/) was used for data preprocessing and analyzing the expression of TRIM22 in the UC (n=6) and control (n=6) groups (GSE59071: 97 UC and 11 control samples; GSE107597: 6 UC samples and 4 control samples). Furthermore, the UCSC database (http://genome.ucsc.edu/) and JASPAR database (http://jaspar.genereg.net/) were used to predict transcriptional binding sites of KLF2 to the TRIM22 promoter.

Cell transfection. Cells ($1x10^5$ cells/well) were seeded into 6-well plates and cultured for 24 h at 37˚C with 5% CO_2. The pGPH1 vector carrying short hairpin (sh)RNA plasmids (sh-TRIM30-1; 5'-CAGTATAGAAGTTACAATA-3' and sh-TRIM30-2; 5'-GGTGAATATCTGTGCACAA-3'), a sh-TRIM22 plasmid (5'-GGAAGATGACATCAGACAA-3'), a sh-KLF2-1 plasmid (5'-GCACCGACGACGACCTCAA-3') and sh-KLF2-2 plasmid (5'-GAAGCGCGGCCGCCGCTCTTG-3'), a negative control (NC) shRNA plasmid (sh-NC), pCDNA3.1 vector targeting KLF2 (Oe-KLF2) and an empty NC vector (Oe-NC) were all purchased from Shanghai GenePharma Co., Ltd. and were dissolved in sterile phosphate-buffered saline (PBS; Beyotime Institute of Biotechnology). Briefly, 70 μl of this solution was gently mixed with 30 μl Lipofectamine® 3000 (Invitrogen; Thermo Fisher Scientific, Inc.) and incubated at room temperature for 20 min to form the complex, according to the manufacturer's protocol. Subsequently, HT-29 cells were seeded in sterile 6-well plates ($1x10^6$ cells/well) at 37˚C and when cell confluence reached ~60%, 200 nM of the complex was transfected into cells. Following transfection for 24 h, DSS was added and cells were incubated for 24 h as aforementioned. Each experiment was performed in triplicate.

TUNEL staining assay. Apoptosis was detected using a TUNEL kit (MilliporeSigma) at 37˚C for 60 min. Cells were washed with PBS and fixed with 40 μl 4% paraformaldehyde for 15 min at room temperature. The cells were then permeabilized in 0.3% Triton X-100/PBS for 10 min, followed by two washes with PBS. After washing, 3% H_2O_2 was added to inhibit endogenous peroxide and 3,3-diaminobenzidine was added to induce color generation at room temperature for 5 min, according to the manufacturer's instructions. 0.5 μg/ml DAPI (Beyotime) was adopted to stain the nuclear for 5 min at room temperature. Antifade Mounting Medium was used to seal the cells. Images of the cells randomly selected from 5 fields of view were captured under an Olympus BX51 fluorescence microscope (Olympus Corporation; magnification, x200).

Animal model. A total of 20 C57BL/6 mice (male; age, 6 weeks; weight, 20-22 g) were purchased from the Medical Comparative Center of Yangzhou University (Yangzhou, China) and were maintained under the following conditions: 55±15% humidity; 26±2˚C; 12-h light/dark cycle; with *ad libitum* access to food and water. The animal experiments performed in the present study were approved by the Ethics Committee of Suzhou Hospital Affiliated to Nanjing Medical University (Suzhou, China). All operations and experimental procedures complied with the Animal Management Regulations of the Ministry of Health (22).

sh-TRIM30 or sh-NC was dissolved in sterile PBS and mixed with Lipofectamine 3000 to form the complex as aforementioned. Mice were randomly assigned into the following four groups (n=5 mice/group): Group I (control), mice were given normal drinking water; Group II [dextran sulphate sodium (DSS)], mice were administered drinking water containing 2% of DSS for 1 week; Group III (DSS + sh-NC), mice were administered 200 μl sh-NC mixture by tail vein injection twice per week for 1 week and were then given drinking water containing 2% DSS for 1 week; Group IV (DSS + sh-TRIM30), mice were administered 200 μl sh-TRIM30 mixture by tail vein injection twice per week for 1 week and were then given drinking water containing 2% DSS for 1 week. The body weights of the mice were recorded daily and disease activity index (DAI) was determined by an investigator blinded to the protocol by scoring the extent of body weight loss, stool hemoccult positivity or gross bleeding, and stool consistency in accordance

with the method described by Kihara *et al* (23). DAI was calculated as follows: DAI=(weight loss score + stool characters score + bleeding score)/3 (24). Subsequently, mice were administered 150 mg/kg sodium pentobarbital intraperitoneally to halt their breathing and cardiac arrest was confirmed. The colon was then dissected, photographed, measured for length. Then, colon tissue was embedded and then cut into 4 μm thick slices, fixed in 4% paraformaldehyde for 15 min at room temperature, before being stained with hematoxylin for 10 min and eosin for 2 min at room temperature. The tissue was observed under an Olympus BX40 light microscope (Olympus Corporation).

Cell Counting Kit-8 (CCK-8) assay. The CCK-8 assay was carried out to evaluate cell viability. Briefly, the transfected cells were inoculated into 96-well plates at a density of $2x10^3$ cells/well, and when cell confluence reached 70-80%, 2% DSS or a moderate amount of sterile water was added and incubated at 37˚C for 24 h. Subsequently, 10 μl CCK-8 solution (Phygene Scientific) was added to each well and the cells were cultured for another 2 h at 37˚C. The absorbance in each well was measured at a wavelength of 450 nm using a microplate reader (BioTek Instruments, Inc.).

Reverse transcription-quantitative PCR (RT-qPCR) analysis. Total RNA (~860 ng/μl) was extracted using TRIzol® reagent (Invitrogen; Thermo Fisher Scientific, Inc.) with a purity of A260/A280 ~1.8, according to the manufacturer's instructions. cDNA was synthesized using the QuantiTect Reverse Transcription kit (Qiagen GmbH) according to the kit's operating procedures. Subsequently, RT-qPCR was performed on an ABI 7500 Real-Time PCR instrument (Applied Biosystems; Thermo Fisher Scientific, Inc.) using the SYBR Green PCR kit (Takara Bio, Inc.), according to the manufacturer's protocol. The reaction system was as follows: 95˚C for 10 min; followed by 40 cycles at 95˚C for 10 sec and 60˚C for 60 sec and final extension at 72˚C for 60 sec. The following primers (GenScript) were used for qPCR: TRIM22, forward 5'-CCGCCTGGAAGATCGAGAG-3' and reverse 5'-CTGCCAGGTTATCCAGCACA-3'; TRIM30, forward 5'-CTCCCAAGAGGACCAGCAC-3' and reverse 5'-ACTCCTCACACTGCAGAGCA-3'; KLF2, forward 5'-ACTCACACCTGCAGCTACGC-3' and reverse 5'-AGTGGTAGGGCTTCTCACCTGT-3'; GAPDH (applicable species: human), forward 5'-GTAGAGCGGCCGCCATGT-3' and reverse 5'-GCCCAATACGACCAAATCAGAGAA-3'; and GAPDH (applicable species: mouse), forward 5'-ACCCTTAAGAGGGATGCTGC-3' and reverse 5'-CCCAATACGGCCAAATCCGT-3'. mRNA expression levels were quantified using the $2^{-\Delta\Delta Cq}$ method (25) and normalized to the internal reference gene GAPDH. Each sample was tested in triplicate and average values were obtained.

Western blot analysis. Cells in each group were collected and RIPA lysis buffer (cat. no. P0013C; Beyotime Institute of Biotechnology) was used to extract total protein. The protein concentration was determined using a BCA protein assay kit (cat. no. P0012S; Beyotime Institute of Biotechnology). Protein samples (20 μg) were separated by 10% SDS-PAGE and then transferred to PVDF membranes soaked in methanol and blocked with 5% bovine serum albumin (Shanghai Rebiosci Biotech Co., Ltd) at room temperature for 30 min. The membranes were then incubated with primary antibodies against TRIM22 (cat. no. ab68071; 1:1,000 dilution; Abcam), TRIM30 (cat. no. ab76972; 1:1,000 dilution; Abcam), NF-κB (cat. no. ab32536; 1:1,000 dilution; Abcam), IκBα (cat. no. 9242S; 1:1,000 dilution; Cell Signaling Technology, Inc.), phosphorylated (p)-NF-κB (cat. no. ab239882; 1:1,000 dilution; Abcam), p-IκBα (cat. no. 2859S; 1:1,000 dilution; Cell Signaling Technology, Inc.), KLF2 (cat. no. ab236507; 1:2,000 dilution; Abcam) and GAPDH (cat. no. ab181602; 1:10,000 dilution; Abcam) at 4˚C overnight. Subsequently, membranes were incubated with horseradish peroxidase-conjugated secondary antibodies (cat. no. 7074, 1:5,000; cat. no. 7076, 1:3,000; both Cell Signaling Technology, Inc.) at room temperature for 2 h. Following the addition of ECL solution (Shanghai Yeasen Biotechnology Co., Ltd.), the protein bands were visualized with a gel imager (C150; Azure Biosystems, Inc.). The gray value of the protein bands was analyzed using ImageJ (v1.51; National Institutes of Health) and the relative protein expression levels were calculated.

Dual-luciferase reporter assay. HT-29 cells were inoculated in a 24-well plate with $1.0x10^5$ cells/well. Once the cell confluence reached 80%, luciferase activity was detected according to the instructions of a dual-luciferase reporter gene assay kit (cat. no. ab228530; Abcam). In brief, the pGL3-KLF2 or pGL3 vector (Promega Corporation) was co-transfected into HT-29 cells together with a luciferase reporter plasmid containing TRIM22 promoter, or mutated TRIM22 promoter using Lipofectamine® 3000 (Invitrogen; Thermo Fisher Scientific, Inc.) in 24-well plates for 24 h, the culture supernatant was discarded, the cells were collected and gently rinsed three times with PBS. Subsequently, 120 μl cell lysis buffer was added to each well of 24-well plates and the plates were agitated on a horizontal oscillator for 45 min at 110 rpm. Fully lysed cell mixture (10 μl) was added to a 1.5 ml microplate well and 50 μl firefly luciferase reagent was added and mixed. Within 10 min, Stop/Glo sealin luciferase reagent (50 μl) was then added, quickly mixed and luciferase activity was measured. Firefly Luc/*Renilla* Luc values were recorded and the TRIM22 promoter transfer activity was analyzed and normalized to *Renilla* luciferase activity. Each group was set up with three multiple wells, and each experiment was repeated three times.

Enzyme-linked immunosorbent assays (ELISAs). The levels of TNF-α (cat. no. PT518), IL-6 (cat. no. P1330) and IFN-γ (cat. no. P1511) in HT-29 cells were quantified using ELISA kits (Beyotime Institute of Biotechnology) according to the manufacturer's instructions.

Chromatin immunoprecipitation (ChIP) assay. Total genomic DNA was isolated and sonicated using the EZChip™ Kit (cat. no. 17-371, MilliporeSigma) according to the manufacturer's protocol. Cell ($4x10^6$ cells/well) were lysed in 400 μl SDS Lysis Buffer (Beyotime Institute of Biotechnology) and then 800 μl cells lysate was sonicated on ice (4.5 sec impact, 9 sec per interval, 14 times in total) and the fragmented DNA was visualized on an agarose gel. Anti-THAP11 (1 μg)

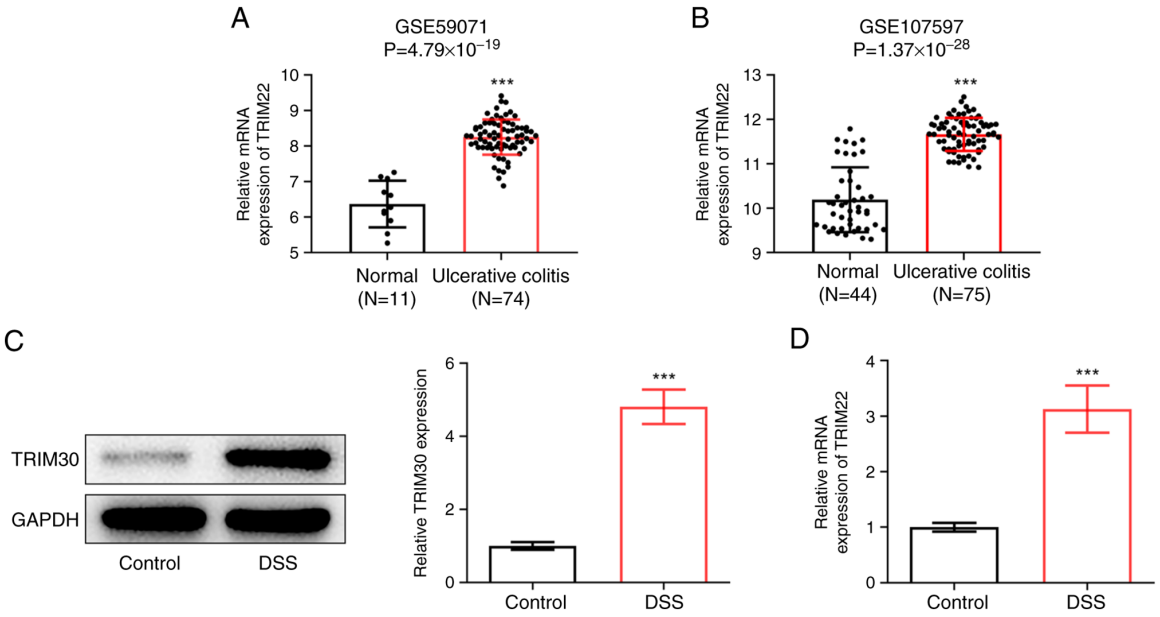

Figure 1. TIRM30 is upregulated in DSS-induced ulcerative colitis in mice. (A and B) GEO2R analysis was used to predict the expression levels of TRIM22 in the intestinal tissues of patients with ulcerative colitis. ***P<0.001 vs. Normal. (C) Western blot analysis and (D) reverse transcription-quantitative PCR were performed to detect the expression levels of TRIM30 in DSS-treated mice. ***P<0.001 vs. Control. DSS, dextran sulphate sodium; TRIM, tripartite motif-containing.

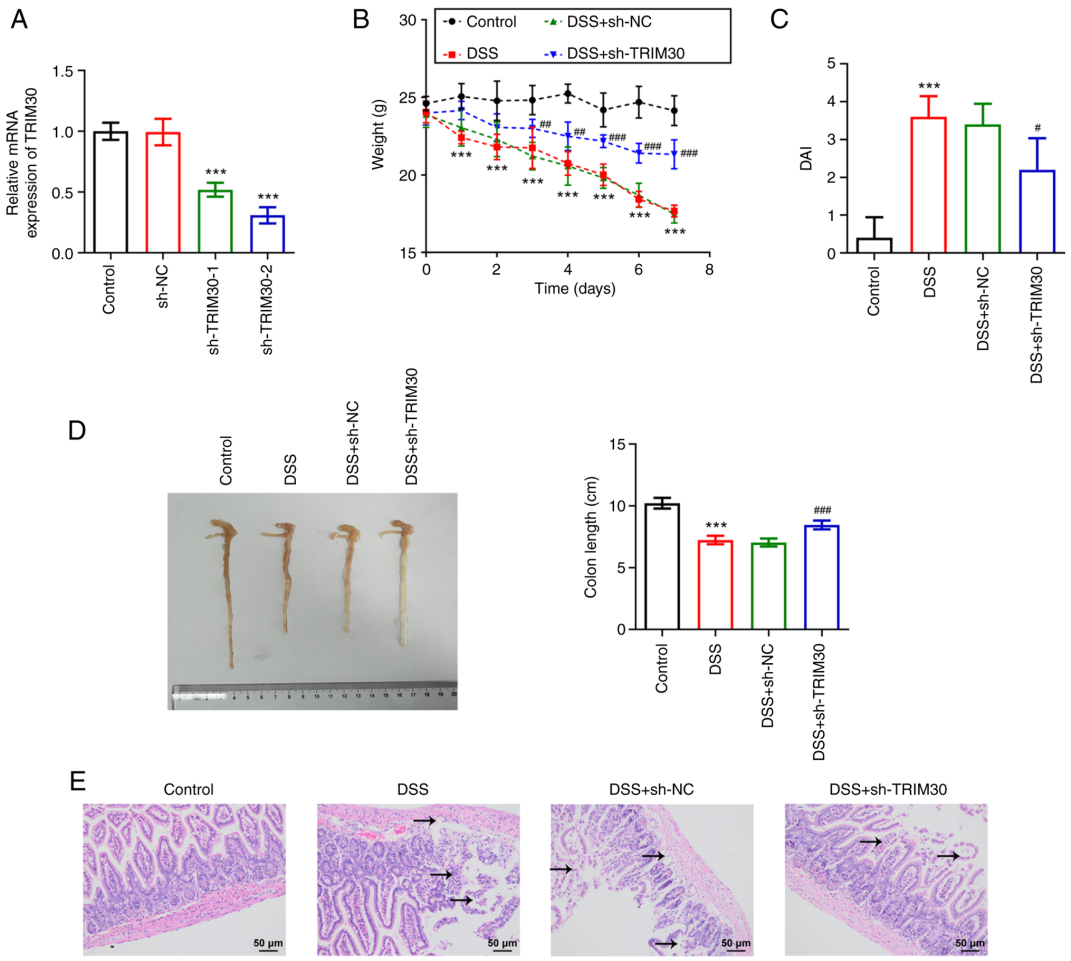

Figure 2. Knockdown of TRIM30 alleviates intestinal injury in a mouse model of DSS-induced ulcerative colitis. (A) Reverse transcription-quantitative PCR was used to detect the mRNA expression levels of TRIM30 in liver tissue. Effects of TRIM30 knockdown on (B) body weight, (C) DAI score and (D) colon length of DSS-treated mice. (E) H&E staining was performed to detect intestinal tissue injury in mice. ***P<0.001 vs. Control; #P<0.05, ##P<0.01 and ###P<0.001 vs. DSS + sh-NC. DAI, disease activity index; DSS, dextran sulphate sodium; NC, negative control; sh, short hairpin; TRIM, tripartite motif-containing.

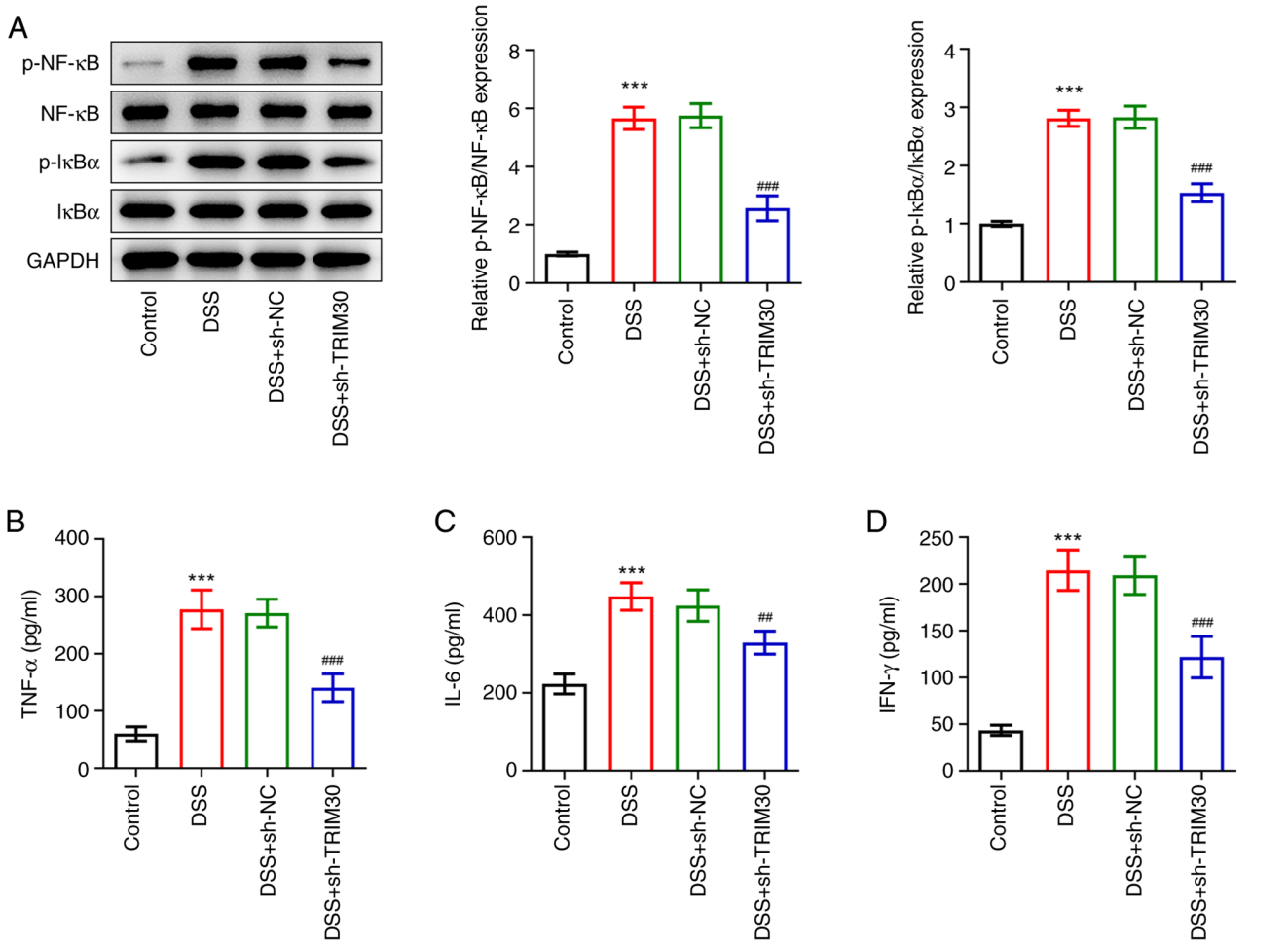

Figure 3. Knockdown of TRIM30 inhibits NF-κB signaling and alleviates inflammation in a mouse model of DSS-induced ulcerative colitis. (A) Expression levels of NF-κB pathway-related proteins (p-NF-κB NF-κB, IκBα and p-IκBα) were detected by western blotting. ELISA was used to detect the levels of (B) TNF-α, (C) IL-6 and (D) IFN-γ. ***P<0.001 vs. Control; ##P<0.01 and ###P<0.001 vs. DSS + sh-NC. DSS, dextran sulphate sodium; NC, negative control; p, phosphorylated; sh, short hairpin; TRIM, tripartite motif-containing.

(cat. no. sc-517366, Santa Cruz Biotechnology, Inc.) or IgG secondary antibodies (Anti-mouse IgG (AS003), ABclonal Technology Co., Ltd.) were added to interact with the target protein-DNA complex. For chromatin isolation, the sample was centrifuged again at 15,000 x g for 10 min at 4˚C to remove insoluble material and 10X ChIP dilution buffer (cat. no. abs50034-22T, Absin Biotechnology Co., Ltd.) was added to the collected supernatant. The sample was pre-cleared with protein G-agarose beads at 4˚C for 1 h with mixing. The samples were centrifuged at 700 x g for 1 min at 4˚C. After boiling, the immunological chromatin samples were amplified by PCR as aforementioned.

Statistical analysis. Data were plotted with GraphPad Prism 8.0 software (GraphPad Software, Inc.). Data are presented as the mean ± standard deviation from ≥3 independent experiments. Unpaired Student's t-test was used for comparisons between two groups, and one-way ANOVA followed by Tukey's post hoc test was used for comparisons among multiple groups. The non-parametric Kruskal-Wallis test was used to analyze the DAI, followed by Dunn's multiple comparison test. P<0.05 was considered to indicate a statistically significant difference.

Results

TRIM30 is upregulated in DSS-induced UC in mice. Firstly, GEO2R analysis was performed on the UC-related datasets GSE59071 (11 control samples, 74 UC samples) and GSE107597 (44 control samples, 75 UC samples); the results revealed that TRIM22 was upregulated in the intestinal tissues of patients with UC (Fig. 1A and B). Subsequently, a mouse model of UC was constructed by induction with 2% DSS, and the expression levels of TRIM30 in DSS-treated mice were detected by western blotting and RT-qPCR. The results showed that the expression levels of TRIM30 were significantly increased in DSS-treated mice compared with those in mice given normal drinking water (Fig. 1C and D).

Knockdown of TRIM30 alleviates intestinal injury in DSS-induced UC in mice. To further explore the role of TRIM30 in UC, sh-TRIM30 was constructed and the knockdown efficiency was verified by RT-qPCR. Compared with sh-TRIM30-1, the knockdown efficiency of the sh-TRIM30-2 plasmid was higher (Fig. 2A); therefore, sh-TRIM30-2 was selected for the subsequent experiments. After 1 week of 2% DSS treatment, the body weight of the DSS group was

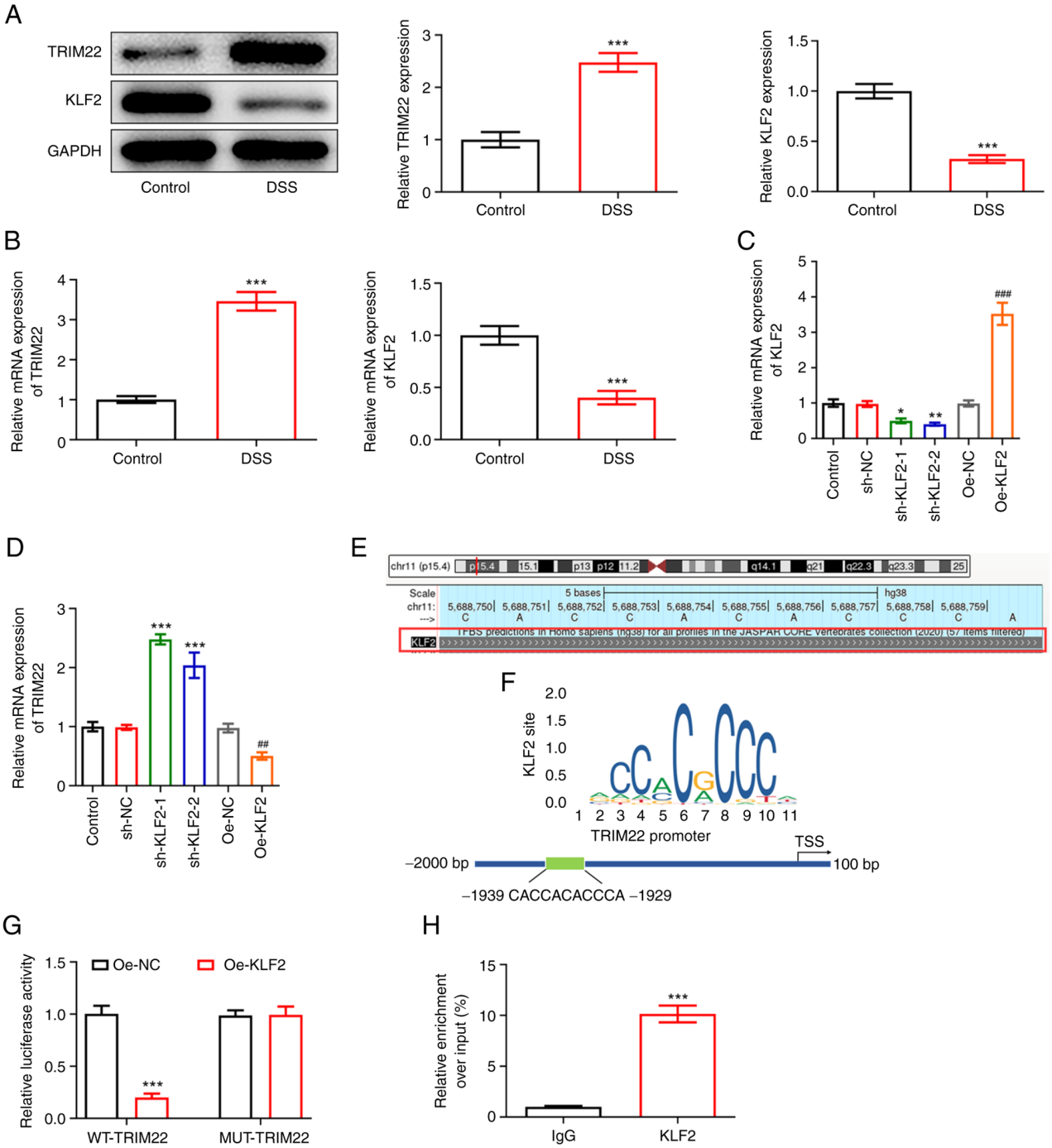

Figure 4. TRIM22 is inhibited by KLF2 transcription in a HT-29 cell model of DSS-induced ulcerative colitis. (A) Western blot analysis and (B) RT-qPCR were used to detect the expression levels of TRIM22 and KLF2 in DSS-treated HT-29 cells. mRNA expression levels of (C) KLF2 or (D) TRIM22 in DSS-treated HT-29 cells transfected with sh-KLF2 or Oe-KLF2, as determined by RT-qPCR. (E) UCSC and (F) JASPAR databases were used to predict the binding site of KLF2 to the TRIM22 promoter. (G) Relative luciferase activity of TRIM22 promoter was detected by luciferase reporter gene assay. (H) Chromatin immunoprecipitation was further used to detect the binding ability of KLF2 to TRIM22. *P<0.05, **P<0.01 and ***P<0.001 vs. Control; $^{\#\#}$P<0.01 and $^{\#\#\#}$P<0.001 vs. Oe-NC. DSS, dextran sulphate sodium; KLF2, Kruppel-like factor 2; Mut, mutant; NC, negative control; Oe, overexpression; RT-qPCR, reverse transcription-quantitative PCR; sh, short hairpin; TRIM, tripartite motif-containing; WT, wild-type.

significantly lower than that of the mice given normal drinking water (Fig. 2B), DAI scores were higher than those of the control group (Fig. 2C) and mice in the DSS group had a shortened colon length with tissue damage (Fig. 2D and E). Notably, knockdown of TRIM30 effectively alleviated the aforementioned inflammatory damage, as evidenced by increased body weight, decreased DAI score, longer colon length and reduced colon tissue damage.

Knockdown of TRIM30 inhibits NF-κB signaling and alleviates inflammation of DSS-induced UC in mice. To verify whether TRIM30 served a pro-inflammatory role through the NF-κB signaling pathway, the expression levels of NF-κB-related proteins were detected by western blotting. Compared with mice in the normal drinking water group, the protein expression levels of p-NF-κB and p-IκBα were significantly increased in DSS-treated mice,

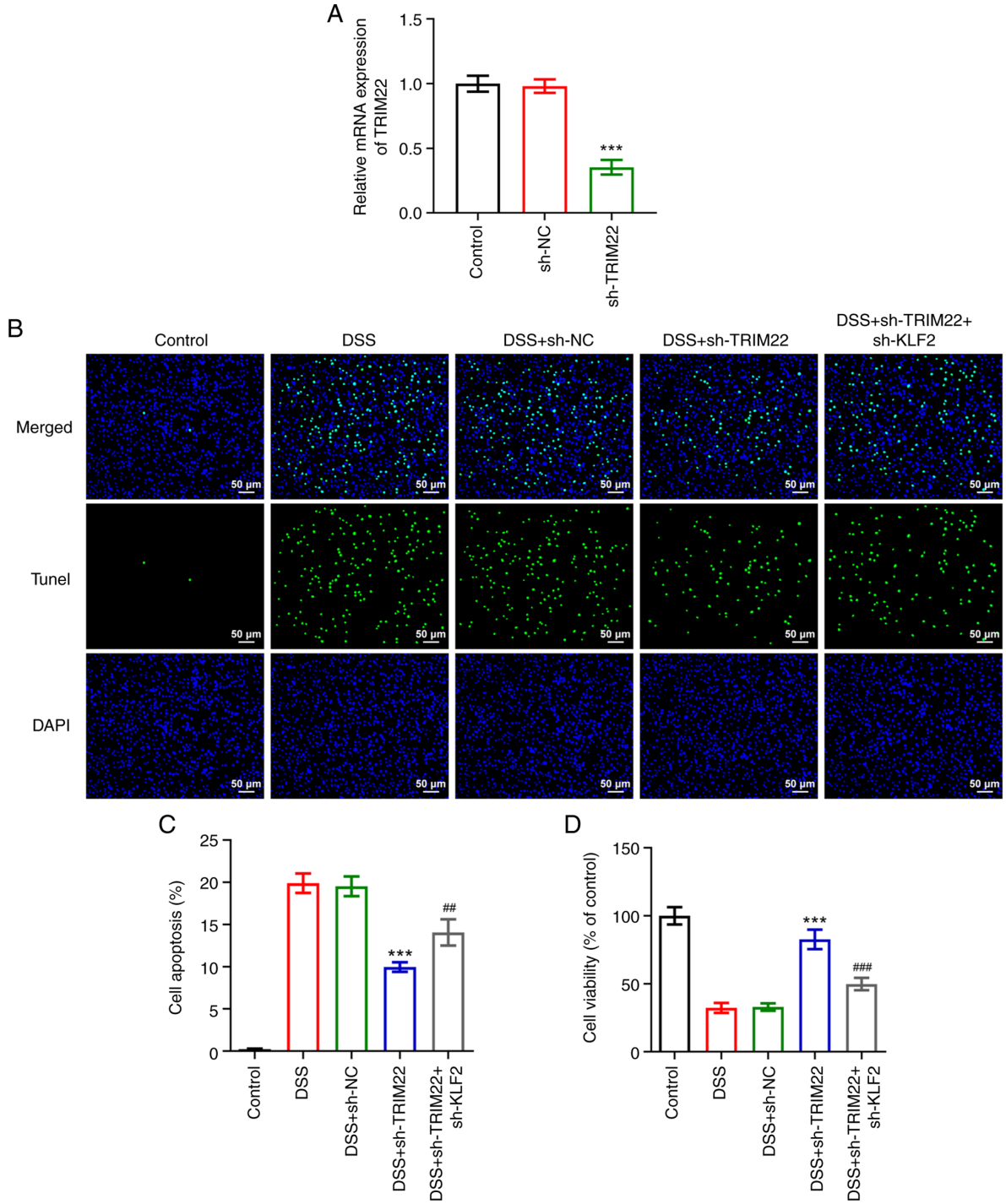

Figure 5. Knockdown of KLF2 reverses the enhancing effects of sh-TRIM22 on viability in DSS-treated HT-29 cells. (A) mRNA expression levels of TRIM22 in HT-29 cells was detected by reverse transcription-quantitative PCR. ***P<0.001 vs. sh-NC. (B and C) TUNEL staining and (D) Cell Counting Kit-8 assay were used to determine the effects of KLF2 and TRIM22 knockdown on apoptosis and viability of DSS-treated HT-29 cells. ***P<0.001 vs. DSS + sh-NC; $^{##}$P<0.01 and $^{###}$P<0.001 vs. DSS + sh-TRIM22. DSS, dextran sulphate sodium; KLF2, Kruppel-like factor 2; NC, negative control; sh, short hairpin; TRIM, tripartite motif-containing.

which was prevented by knockdown of TRIM30 (Fig. 3A). In addition, the levels of inflammation-related factors (TNF-α, IL-6 and IFN-γ) were examined by ELISA. As shown in Fig. 3B-D, DSS induced an increase in TNF-α, IL-6 and IFN-γ levels in mice, by contrast, the levels of inflammation-related factors were significantly decreased following TRIM30 knockdown, effectively alleviating the inflammatory response in mice.

TRIM22 is inhibited by KLF2 in DSS-induced UC in HT-29 cells. Firstly, the expression levels of TRIM22 and KLF2 were detected in DSS-treated HT-29 cells by western blotting and RT-qPCR. Compared with in the control group, the mRNA and protein expression levels of TRIM22 were significantly upregulated in DSS-induced HT-29 cells, whereas the expression levels of KLF2 were significantly downregulated (Fig. 4A and B). Subsequently, an overexpression vector and a knockdown

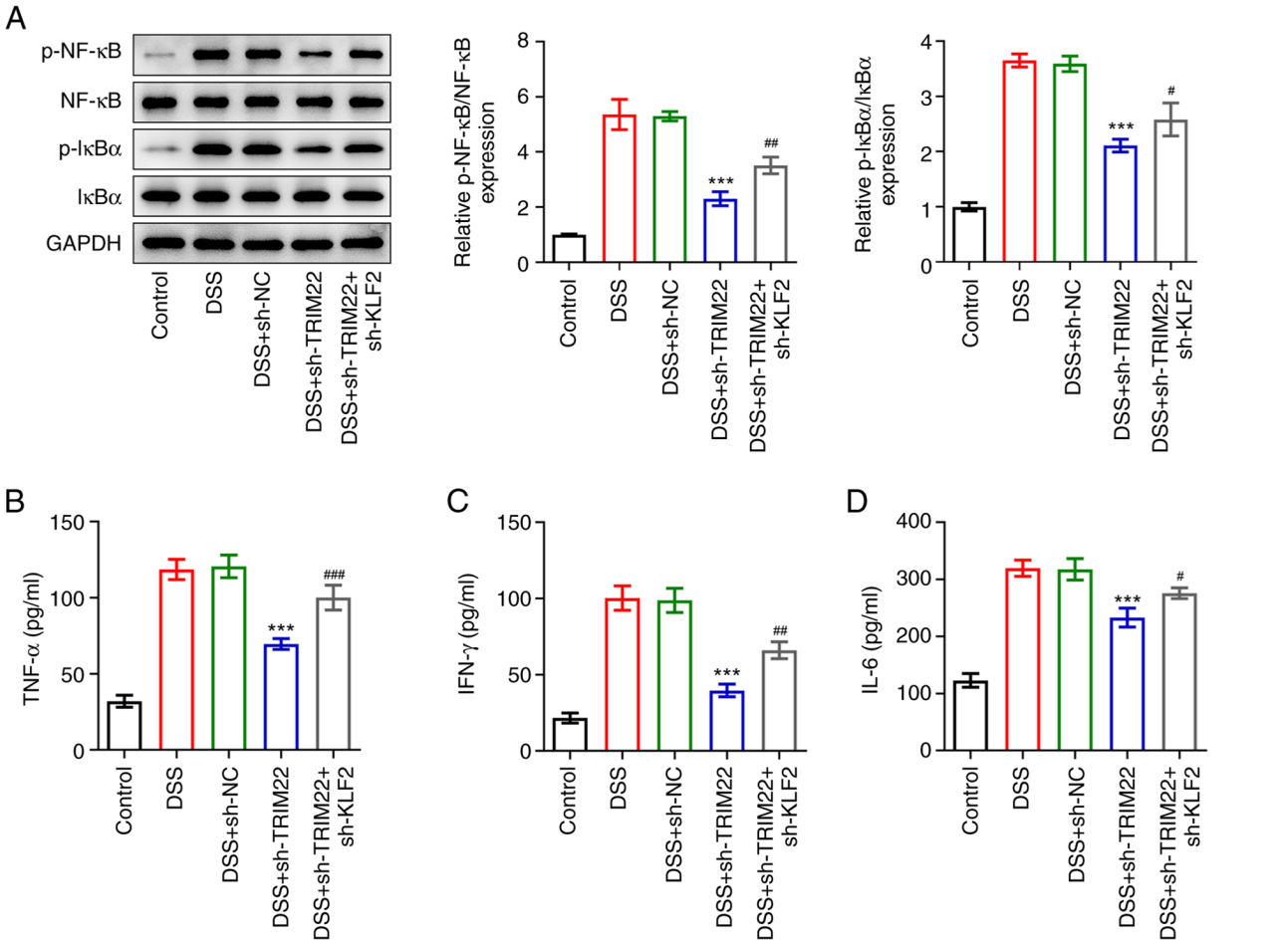

Figure 6. Knockdown of KLF2 reverses the inhibitory effects of sh-TRIM22 on NF-κB signaling and inflammation in DSS-treated HT-29 cells. (A) Expression levels of NF-κB pathway-related proteins (p-NF-κB NF-κB, IκBα and p-IκBα) were detected by western blotting. ELISA was used to detect the levels of (B) TNF-α, (C) IL-6, and (D) IFN-γ. ***P<0.001 vs. DSS + sh-NC; $^{\#}$P<0.05, $^{\#\#}$P<0.01 and $^{\#\#\#}$P<0.001 vs. DSS + sh-TRIM22. DSS, dextran sulphate sodium; KLF2, Kruppel-like factor 2; NC, negative control; p, phosphorylated; sh, short hairpin; TRIM, tripartite motif-containing.

vector of KLF2 were constructed, and transfection efficiency was detected by RT-qPCR. The results revealed that following transfection with oe-KLF2 and sh-KLF2-1/2, the expression levels of KLF2 were significantly increased or decreased, respectively (Fig. 4C). sh-KLF2-2 had a better transfection effect than sh-KLF2-1, and was selected for the next experiments. Subsequently, the expression levels of TRIM22 were detected and it was revealed that after knockdown of KLF2, the expression levels of TRIM22 were significantly promoted. By contrast, following overexpression of KLF2, the expression levels of TRIM22 were significantly inhibited (Fig. 4D), indicating that TRIM22 was possibly inhibited by KLF2 transcription. The present study therefore aimed to further explore the relationship between TRIM22 and KLF2. The results obtained from UCSC and JASPAR databases implicated that KLF2 could bind to the TRIM22 promoter sequence (Fig. 4E and F). Luciferase activity assay results demonstrated that overexpression of KLF2 significantly inhibited the luciferase activity of the TRIM22-wild-type reporter plasmid, but had no effect on the luciferase activity of the TRIM22-mutant reporter plasmid (Fig. 4G). Furthermore, the CHIP assay demonstrated that KLF2 could bind the TRIM22 promoter (Fig. 4H). Therefore, these results indicated that KLF2 could bind to the TRIM22 promoter to inhibit the expression of TRIM22.

Knockdown of KLF2 reverses the effects of sh-TRIM22 on viability, NF-κB signaling and inflammation in DSS-treated HT-29 cells. The present study evaluated the effect of the relationship between KLF2 and TRIM22 on UC. RT-qPCR assay demonstrated that the expression levels of TRIM22 were significantly decreased in HT-29 cells post-transfection with sh-TRIM22 (Fig. 5A). Subsequently, TUNEL staining and CCK-8 were used to assess the apoptosis and viability of cells. The results revealed that TRIM22 knockdown could significantly inhibit DSS-induced apoptosis and viability; however, this effect was reversed by further interference with KLF2 (Fig. 5B-D). As previously reported, sh-TRIM22 markedly inhibited the expression levels of NF-κB pathway-related proteins and inflammation-related factors (Fig. 3A and B). Notably, the present study interfered with KLF2 *in vitro* and demonstrated that sh-KLF2 reversed the inhibitory effect of sh-TRIM22 on the levels of NF-κB signaling pathway proteins (Fig. 6A) and inflammatory factors (Fig. 6B-D) in DSS-treated HT-29 cells.

Discussion

UC is a chronic non-specific inflammatory bowel disease, which mainly occurs in the intestinal mucosa and

submucosa (1). UC is characterized by long-term disease, recurrence and the risk of cancer, which seriously affects the quality of life of patients (3,26). In recent years, evidence has suggested that variations in TRIM22 expression may be related to inflammatory bowel disease (27). Overexpression of TRIM22 has been shown to inhibit the growth of monocytes, whereas downregulation of TRIM22 could protect neurons against oxygen-glucose deprivation/re-oxygenation-induced apoptosis and inflammation (11). The present study revealed that TRIM30 was upregulated in an *in vivo* model of UC and knockdown of TRIM30 alleviated DSS-induced intestinal injury in mice with UC.

The NF-κB pathway has long been considered a typical pro-inflammatory signaling pathway (28). It has been reported that TRIM22 may be used as a potential activator of the NF-κB signaling pathway (29). Notably, TRIM22 has been shown to activate the NF-κB signaling pathway by increasing degradation of the NF-κB inhibitor IκBα (29). Kang *et al* (11) revealed that knocking down TRIM22 alleviated inflammation and apoptosis induced by cerebral ischemia-reperfusion by inhibiting the NF-κB/NLRP3 axis. Therefore, the present study examined the expression levels of NF-κB pathway-associated proteins and inflammatory factors in a model of UC. The results indicated that knockdown of TRIM30 significantly inhibited NF-κB signaling and alleviated DSS-induced intestinal inflammation in mice with UC, which was consistent with the findings of Kang *et al* (11), suggesting that TRIM30 may induce inflammation through activation of the NF-κB pathway.

The present study also assessed the mechanism underlying the effects of TRIM22 on UC and it was revealed that KLF2, as the upstream transcription factor of TRIM22, could effectively bind to the TRIM22 promoter sequence according to bioinformatics analysis. This finding was confirmed by dual-luciferase reporter assay and ChIP. Since TRIM22 induced inflammation by activating NF-κB, given the association of KLF2 with TRIM22 promoter binding, it is hypothesized that KLF2 also regulates inflammation, which is consistent with previous studies on the regulatory role of KLF2 in various inflammatory diseases (17,30). According to the results of a previous study, KLF2 could serve a regulatory role in acute lung injury as a transcription inhibitor of HSPH1 (18). In addition, simvastatin has been reported to upregulate the expression of KLF2 in vascular endothelial cells susceptible to atherosclerosis and relieve vascular inflammation (31). These results indicated that KLF2 and TRIM22 may have opposite regulatory roles in UC; therefore, the cells were co-transfected with sh-TRIM22 and sh-KLF2. Notably, KLF2 knockdown inhibited cell viability, promoted apoptosis, and enhanced NF-κB signaling and inflammation in DSS-treated HT-29 cells transfected with sh-TRIM22. These results indicated that TRIM22 may have a role in promoting disease progression by activating the NF-κB signaling pathway in UC but could be inhibited by its upstream transcription factor KLF2.

In conclusion, DSS significantly increased the expression levels of TRIM22 in HT-29 cells and TRIM30 in mice, whereas KLF2 knockdown reversed the inhibitory effect of TRIM22 on viability and the enhancing effects of TRIM22 on inflammation in DSS-treated HT-29 cells. These results suggested that TRIM22 and KLF2 may be potential targets for the treatment of UC, and also provided information that may improve the understanding of the pathogenesis of UC.

Acknowledgements

Not applicable.

Funding

The present study was supported by the Project and the Suzhou Science and Technology Development Plan Project (grant no. 2018.55).

Availability of data and materials

The datasets used and/or analyzed during the current study are available from the corresponding author on reasonable request.

Authors' contributions

BY and ZL conceptualized and designed the current study. BY acquired, analyzed and interpreted the data. ZL drafted the manuscript and revised it critically for important intellectual content. Both authors agreed to be held accountable for the current study in ensuring questions related to the integrity of any part of the work are appropriately investigated and resolved. BY and ZL confirm the authenticity of all the raw data. Both authors read and approved the final manuscript.

Ethics approval and consent to participate

Animal experiments in the present study were approved by the Ethics Committee of Suzhou Hospital affiliated to Nanjing Medical University.

Patient consent for publication

Not applicable.

Competing interests

The authors declare that they have no competing interests.

References

1. Adams SM and Bornemann PH: Ulcerative colitis. Am Fam Physician 87: 699-705, 2013.
2. Keshteli AH, Madsen KL and Dieleman LA: Diet in the pathogenesis and management of ulcerative colitis; a review of randomized controlled dietary interventions. Nutrients 11: 1498, 2019.
3. Du L and Ha C: Epidemiology and pathogenesis of ulcerative colitis. Gastroenterol Clin North Am 49: 643-654, 2020.
4. Kaenkumchorn T and Wahbeh G: Ulcerative colitis: Making the diagnosis. Gastroenterol Clin North Am 49: 655-669, 2020.
5. da Silva BC, Lyra AC, Rocha R and Santana GO: Epidemiology, demographic characteristics and prognostic predictors of ulcerative colitis. World J Gastroenterol 20: 9458-9467, 2014.
6. Huang Y, Chen J, Wong T and Liow JL: Experimental and theoretical investigations of non-Newtonian electro-osmotic driven flow in rectangular microchannels. Soft Matter 12: 6206-6213, 2016.
7. Nowarski R, Jackson R, Gagliani N, de Zoete MR, Palm NW, Bailis W, Low JS, Harman CC, Graham M, Elinav E and Flavell RA: Epithelial IL-18 equilibrium controls barrier function in colitis. Cell 163: 1444-1456, 2015.

8. Pugliese D, Felice C, Papa A, Gasbarrini A, Rapaccini GL, Guidi L and Armuzzi A: Anti TNF-α therapy for ulcerative colitis: Current status and prospects for the future. Expert Rev Clin Immunol 13: 223-233, 2017.
9. Li L, Qi Y, Ma X, Xiong G, Wang L and Bao C: TRIM22 knockdown suppresses chronic myeloid leukemia via inhibiting PI3K/Akt/mTOR signaling pathway. Cell Biol Int 42: 1192-1199, 2018.
10. Lou J, Wang Y, Zheng X and Qiu W: TRIM22 regulates macrophage autophagy and enhances *Mycobacterium tuberculosis* clearance by targeting the nuclear factor-multiplicity κB/beclin 1 pathway. J Cell Biochem 119: 8971-8980, 2018.
11. Kang C, Lu Z, Zhu G, Chen Y and Wu Y: Knockdown of TRIM22 relieves oxygen-glucose deprivation/reoxygenation-induced apoptosis and inflammation through inhibition of NF-κB/NLRP3 axis. Cell Mol Neurobiol 41: 341-351, 2021.
12. Li Q, Lee CH, Peters LA, Mastropaolo LA, Thoeni C, Elkadri A, Schwerd T, Zhu J, Zhang B, Zhao Y, *et al*: Variants in TRIM22 that affect NOD2 signaling are associated with very-early-onset inflammatory bowel disease. Gastroenterology 150: 1196-1207, 2016.
13. Liu R, Zhao W, Wang H and Wang J: Long noncoding RNA LINC01207 promotes colon cancer cell proliferation and invasion by regulating miR-3125/TRIM22 axis. Biomed Res Int 2020: 1216325, 2020.
14. Chen C, Zhao D, Fang S, Chen Q, Cheng B, Fang X and Shu Q: TRIM22-mediated apoptosis is associated with bak oligomerization in monocytes. Sci Rep 7: 39961, 2017.
15. Ji F and Sadreyev RI: RNA-seq: Basic bioinformatics analysis. Curr Protoc Mol Biol 124: e68, 2018.
16. Canzoneri R, Lacunza E and Abba MC: Genomics and bioinformatics as pillars of precision medicine in oncology. Medicina (B Aires) 79 (Spec 6/1): 587-592, 2019.
17. Wang ZL, Wang YD, Wang K, Li JA and Li L: KFL2 participates in the development of ulcerative colitis through inhibiting inflammation via regulating cytokines. Eur Rev Med Pharmacol Sci 22: 4941-4948, 2018.
18. Liang Y, Luo J, Yang N, Wang S, Ye M and Pan G: Activation of the IL-1β/KLF2/HSPH1 pathway promotes STAT3 phosphorylation in alveolar macrophages during LPS-induced acute lung injury. Biosci Rep 40: BSR20193572, 2020.
19. Vanhove W, Peeters PM, Staelens D, Anica S, der Goten JV, Cleynen I, De Schepper S, Van Lommel L, Reynaert NL, Schuit F, *et al*: Strong upregulation of AIM2 and IFI16 inflammasomes in the mucosa of patients with active inflammatory bowel disease. Inflamm Bowel Dis 21: 2673-2682, 2015.
20. Ouahed J, Gordon W, Canavan JB, Zhou HY, Du S, von Schack D, Phillips K, Wang L, Dunn WA III, Field M, *et al*: Mucosal gene expression in pediatric and adult patients with ulcerative colitis permits modeling of ideal biopsy collection strategy for transcriptomic analysis. Inflamm Bowel Dis 24: 2565-2578, 2018.
21. Cheng F, Li Q, Wang J, Zeng F, Wang K and Zhang Y: Identification of differential intestinal mucosa transcriptomic biomarkers for ulcerative colitis by bioinformatics analysis. Dis Markers 2020: 8876565, 2020.
22. Cardon AD, Bailey MR and Bennett BT: The animal welfare act: From enactment to enforcement. J Am Assoc Lab Anim Sci 51: 301-305, 2012.
23. Kihara N, de la Fuente SG, Fujino K, Takahashi T, Pappas TN and Mantyh CR: Vanilloid receptor-1 containing primary sensory neurones mediate dextran sulphate sodium induced colitis in rats. Gut 52: 713-719, 2003.
24. Chen Q, Fang X, Yao N, Wu F, Xu B and Chen Z: Suppression of miR-330-3p alleviates DSS-induced ulcerative colitis and apoptosis by upregulating the endoplasmic reticulum stress components XBP1. Hereditas 157: 18, 2020.
25. Livak KJ and Schmittgen TD: Analysis of relative gene expression data using real-time quantitative PCR and the 2(-Delta Delta C(T)) method. Mehods 25: 402-408, 2001.
26. Yamamoto-Furusho JK, Gutiérrez-Grobe Y, López-Gómez JG, Bosques-Padilla F, Rocha-Ramírez JL and Grupo del Consenso Mexicano de Colitis Ulcerosa Crónica Idiopática: The Mexican consensus on the diagnosis and treatment of ulcerative colitis. Rev Gastroenterol Mex (Engl Ed) 83: 144-167, 2018 (In English, Spanish).
27. Ashton JJ, Mossotto E, Stafford IS, Haggarty R, Coelho TAF, Batra A, Afzal NA, Mort M, Bunyan D, Beattie RM and Ennis S: Genetic sequencing of pediatric patients identifies mutations in monogenic inflammatory bowel disease genes that translate to distinct clinical phenotypes. Clin Transl Gastroenterol 11: e00129, 2020.
28. Lawrence T: The nuclear factor NF-kappaB pathway in inflammation. Cold Spring Harb Perspect Biol 1: a001651, 2009.
29. Ji J, Ding K, Luo T, Zhang X, Chen A, Zhang D, Li G, Thorsen F, Huang B, Li X and Wang J: TRIM22 activates NF-κB signaling in glioblastoma by accelerating the degradation of IκBα. Cell Death Differ 28: 367-381, 2021.
30. Jha P and Das H: KLF2 in regulation of NF-κB-mediated immune cell function and inflammation. Int J Mol Sci 18: 2383, 2017.
31. Zhuang T, Liu J, Chen X, Zhang L, Pi J, Sun H, Li L, Bauer R, Wang H, Yu Z, *et al*: Endothelial Foxp1 suppresses atherosclerosis via modulation of Nlrp3 inflammasome activation. Circ Res 125: 590-605, 2019.

This work is licensed under a Creative Commons Attribution-NonCommercial-NoDerivatives 4.0 International (CC BY-NC-ND 4.0) License.